Energy & Buildings 278 (2023) 112646

Contents lists available at ScienceDirect

Energy & Buildings

journal homepage: www.elsevier.com/locate/enb

Thermal performance analysis of an existing building heating based on a novel active phase change heater

Zhaoli Zhang [a,*], Nan Zhang [a], Yanping Yuan [a], Patrick E. Phelan [b], Shady Attia [c]

[a] School of Mechanical Engineering, Southwest Jiaotong University, Chengdu 610031, China
[b] School for Engineering of Matter, Transport & Energy, Arizona State University, Tempe 85287-6106, United States
[c] Sustainable Building Design Lab, Dept. UEE, Faculty of Applied Sciences, University of Liège, Liège 4000, Belgium

ARTICLE INFO

Article history:
Received 5 October 2022
Revised 31 October 2022
Accepted 7 November 2022
Available online 11 November 2022

Keywords:
Phase change material
Building heating
Temperature control
Finite element method
Heat transfer characteristic

ABSTRACT

An active phase change heater is configurated to transform excess electricity at off-peak tariff periods into thermal energy, store and release it at the electricity on-peak tariff periods in order to accomplish heating demand towards an existing building with marine climate. Reliable numerical model is developed based on phase change heat transfer and convective heat transfer between phase change material (PCM) and indoor air. Objective temperature zone (18–24 °C) is achieved by means of an event control that is coupled with heat transfer model. Performance of indoor temperature, phase change characteristics and operating model of active phase change heaters during the building heating period are comprehensively evaluated. Results indicate that indoor temperatures are generally within thermal comfort range under various initial temperatures and air inlet velocities. Start-stop frequencies of PCM system increase while total working times decrease with the augment of air velocity. Liquid fractions of PCM decrease as studied time elapses and several parallel stages occur owing to intermittent operation of active phase change heaters. Parametric analysis reveals that thermal resistance is determined as the most decisive factor, followed by ambient temperature, PCM melting point and PCM thermal conductivity. Liquid fraction of PCMs declines to merely 0.074 when thermal resistance increases to 0.4 ($m^2.^oC$)/W. In conclusion, studied results highlight correlation between building thermal performance and specific heat transfer characteristics of PCM, with substantial benefits to development of latent heat thermal energy storage available to building energy conservation.

1. Introduction

Building field accounts for over 30 % of worldwide energy consumption and this situation is increasingly becoming prominent with the improvement of thermal comfort requirements [1]. It is believed that available energy directly or indirectly extracted from fossil fuels will still dominate the global energy market in short term [2]. While, shortages of fossil fuels combining with the environmental issues including global warming, acid rain and smog, etc. continue to deteriorate under this circumstance [3]. Therefore, various possible strategies are urgent to be advanced to address the above energy and environmental issues.

Numerous countries and areas have proclaimed policies to enhance energy utilization efficiency and reduce CO_2 emissions in buildings [4,5]. Thermal energy storage is reckoned as one of feasible approaches. It is generally considered that thermal energy storage can be classified as sensible heat, latent heat, and thermochemical storage [6]. Latent heat thermal energy storage (LHTES, also known as phase change thermal energy storage) employs PCM to achieve heat storage and release during its reversible phase transition [7]. In comparison to others, LHTES shows the incomparable advantages of high energy storage density, nearly isothermal temperature in the phase transition. Thus, it is established that LHTES can be applied in extensive energy fields related to buildings. Overcoming the unstable energy output from solar radiation or other energy sources, LHTES enables to improve the energy utilization efficiency. LHTES also takes full advantage of low-cost electricity at off-peak hours to achieve the peak load shifting that then decreases the cost of maintaining building thermal environment [8,9].

Energy consumption in buildings comes from heating, cooling, lighting and ventilation, which largely depends on the geographical locations, building types and climates. According to the specific working principle, LHTES integrated into the building energy con-

* Corresponding author.
E-mail address: zzlyzhang@outlook.com (Z. Zhang).

https://doi.org/10.1016/j.enbuild.2022.112646
0378-7788/

servation can be categorized into passive and active applications [10,11].

(1) Passive applications.

LHTES can be distributed in various components of passive buildings. Selected PCMs increase thermal mass of the building components, which then availably reduces heat transfer rate between the buildings and ambient environment. Furthermore, this effect can bring to decline of the peak heating or cooling load of the building. Passive applications of LHTES are also beneficial to weaken effects of ambient temperature fluctuations on building components, and therefore result in slighter variations of indoor temperature contrast to no-PCM cases. Several researches associated with passive applications of LHTES have been conducted and normally they can be separated into: PCM walls; PCM roofs or ceilings; PCM floors; PCM windows and solar chimneys with PCM

Bondareva et al. [12] investigated heat transfer process of a building element containing a cavity filled with PCM under non-stationary external thermal effect. It was indicated that the tilt angle of the building block determined the intensity of heat transfer and PCM walls transmitted more heat than PCM roof. Khdair et al. [13] evaluated the reduction of energy demand in the building through the installation of PCM. Heat transfer was calculated transiently on the inner surface of the envelopes and the building performance were reported monthly and annually. Results showed that PCM was effective in July, August and September rather other months. Zhang et al. [14] proposed an innovative reversible multiple-glazing roof integrated with two PCMs to improve thermal performance of a traditional building envelope. The influence of melting temperature and thickness proportion of PCMs on thermal performance of the roof and an energy-economy comparison between the new roof and the traditional roof in full life was investigated. Results indicated that the new glazed roof could provide better energy saving rate in winter than summer. Elawady et al. [15] conducted long-term thermal behavior of building roof containing PCM layer. The roof with and without PCM layer and roof with three different PCMs and three thicknesses were compared at variable outside weather conditions. Results indicated that using PCM in the roof structure decreased the indoor heat flux and interior wall temperature was closer to the indoor air temperature. Bogatu et al. [16] investigated the performance of novel macro-encapsulated PCM as a ceiling cooling component compared to commercially available radiant cooling technologies. The installed heat storage capacity was enough to shift the cooling demand to off-peak periods when the PCM was fully discharged.

In addition to the conventional building envelopes, other possible building components are also taken into consideration and several researches have been carried out to explore the PCM potential applications, including slabs, windows and solar chimneys, etc. Royon at al. [17] described a new component derived from an existing slab that has cylindrical cavities filled with PCMs. Heat transfer of the slab submitted to temperature cyclic conditions and annular repartition for different percentages of PCM were studied. The optimal amount of PCM was determined with analysis of an indicator that was utilized to evaluate the working part of PCM during the thermal cycle. Goia et al. [18] exposed paraffin wax to real solar conditions in a PCM glazing system. Evolution of chemical and physical properties of the paraffin wax were studied and stability was observed in terms of latent heat of fusion after the ageing process. It was observed that maximal decrease of nominal melting temperature was in line with literature data and thermal cycling degradation was possibly caused by the chain structure with formation of aggregated particles. Li et al. [19] experimentally investigated thermal performance of a PCM based solar chimney under various laboratory conditions. Results indicated that the phase change periods were nearly identical for three heat fluxes. The air flow rates varied in correspondence with the absorber surface temperatures. The maximum air flow rate was determined as 0.04 kg/s in the case of 700 W/m^2. While, 500 W/m^2 generated the highest average outlet temperature of 20.35 °C. Dordelly et al. [20] investigated the impact of integrating PCM on the performance of two different solar chimney prototypes with purpose of providing constant ventilation and improving air quality. Results revealed that PCM integration provided a higher ventilation rate when the lamps supplied neglectable energy to the solar chimney.

Based on the aforementioned reviews, it is obtained that extensive literatures related to PCM passively packaged in building envelopes are retrievable from perspectives of experimental and numerical investigations. Corresponding results well testify that LHTES can be a superior strategy to deal with the building energy issue.

(2) Active applications.

Available building energy can derive from electricity, residual thermal energy or a variety of renewable sources, such as solar radiation, air and geothermal energy, etc. It is certificated that integrating LHTES into these building energy systems is one of the possible methods to solve the problems of high cost and unstable outputs [21]. Considering passive modes are usually unable to realize satisfied response between transient energy supply and demand from buildings, adoption of driving devices to make the systems operate in active mode is believed as an practical approach [22]. Actually, active composite systems possess dual functions of quickly gaining thermal energy from selected heat sources and temporarily store them for reuse later. According to the heat generation, active applications can be classified as: solar heating-latent heat system, heat pump-latent heat system and electrical heating-latent heat system.

Stritih et al. [23] utilized LHTES with a hot air solar energy collector mounted on the facade of an office building to heat ventilation air accounting for significant energy conservation. Results showed that the highest coverage ratio of ventilation heat loss was in the transitional period between seasons. Charvát et al. [24] employed PCM for thermal energy storage in air-based solar thermal systems. The CSM panels with RT42 were investigated by means of experimental and numerical tests. Both results indicated that latent heat thermal storage could be employed in extensive systems as a peak shaving measure. Mazo et al. [25] developed a radiant floor system with PCM in simple building types. It was found that the radiant floor with PCM was able to meet the heating demand requirement with a practically total shift of electric energy consumption from the peak period to the off-peak demand times. Oruc et al. [26] analyzed the utilization of a renewable energy-based system with the latent heat storage option for building thermal management. Results showed that the overall energy and exergy efficiencies of the PCM-free radiant heating system were much lower than the case with the PCM-embedded radiant heating system. Benli et al. [27] developed a ground source heat pump-PCM latent heat storage system for thermal environment control of greenhouses. The average heating COP of the ground-source heat pump unit and the overall system COP were obtained in high range which presented that utilization of a ground-source heat pump-PCM system was a suitable approach for greenhouse heating. Lin et al. [28] proposed a novel under-floor electric heating system with shape-stabilized PCM plates. This system charged heat by using cheap nighttime electricity and discharged the stored heat

at daytime. Results indicated that upper surface temperature of the PCM plates could be kept near the phase transition temperature in whole day with obviously low electricity tariff.

Available investigation concerning active application of PCM also has been widely carried out in numerical analysis. Faraj et al. [29] integrated coconut oil with a quarter-scale insulated prototype of an underfloor heating system. Versatility of the underfloor system with PCM facilitated a reduction in heating load during winter while maintaining residential thermal comfort. Results indicated that PCM provided a shift in electricity consumption from peak time to off-peak time with a substantial annual cost reduction compared the control test. Geometric design of solar-aided latent heat storage is theoretically developed based on various parameters and PCMs [30]. Two models were used to describe the diurnal transient behavior of phase change unit. Effects of various PCMs, cylinder radius, pipe dimension, total PCM volume, mass flow rate and inlet temperature of heat transfer fluid (HTF) were assessed in numerical test. Esen et al. [31] built a model to investigate performance of a solar assisted cylindrical energy storage tank. Transient behavior of phase change unit was measured and the heat storage capacities of different PCMs were compared. Results showed that optimization of the tank should be conducted from PCM, cylinder radius, the mass flow rate, and the inlet temperature of HTF. A cylindrical phase change storage tank was also linked to a solar powered heat pump system [32]. The research was performed to measure the mean temperature of water within the tank and the inlet and outlet temperature of the tank. They also presented solar radiation and space heating loads for the heating seasons. Qiao et al. [33] conducted a study to reveal thermal performance and energy efficiency of an active solar heating wall coupled with PCM system. Four impact factors including number and location of water capillary pipes, PCM wallboard thickness and heating water temperature were analyzed. Test room with the built system achieved an energy conservation of 1.93 kWh and an indoor temperature of 21.9 °C, which were higher than that of the reference room. Kong et al. [34] configured a solar collector integrated with PCM system to make full use of renewable energy for building heating. Feasibility and economic efficiency of the system in practical applications were studied. Results displayed that the area of solar collector had the greatest impact on indoor temperature, while the power of electric heating furnace had the greatest impact on the levelized cost of heat.

It is concluded that active applications of PCM enable to complete the fast switching between thermal energy storage and release, in response to demand of building energy consumption. Whereas, to our best knowledge, there are few studies concerned dynamic response relationship between indoor thermal environment and transient thermal and mass performance of LHTES applied in buildings, especially for existing buildings located in the Belgium regions with marine climate where are unsuitable for large-scale reconstruction and retrofit. Since their heating demands are much larger than cooling, passive LHTES is unable to accomplish the heavy load demand of these buildings [15,25]. Therefore, this paper designs a novel active LHTES that utilizes the abundant electricity at off-peak tariff periods as heat source. The stored thermal energy can be discharged into the indoor environment at on-peak tariff periods in an active operating form. Taking full advantage of electrical price difference between peak and valley hours, the proposed phase change heater enables to provide a possible strategy to reduce the cost of building heating. The daily thermal performance of indoor environment and phase change characteristics of PCM during the discharging process at on-peak tariff periods (assuming 900 min) are conducted based on built theoretical model. The operating models of active phase change heaters including start-stop frequency, first run time and total working time are also measured. In addition, parametric analysis is explicitly studied to reveal effects of several important factors on system performance.

2. Numerical investigation

2.1. Physical model

A two-dimensional physical model is developed to evaluate performance of a building integrated with an active phase change heater, as shown in Fig. 1. The building is specified as a rectangular with detailed length (L_b) and height (H_0 + H_b) of 4 m and 3 m, respectively. It is observed that the active phase change heater is installed in the lower left part of a building. A substantial distance of 200 mm above the floor is reserved for installing the active phase change heater. Specification of the active phase change heater is indicated in Fig. 1 and it is revealed that air channel placed into the center of the active phase change heater is made of thin copper sheets. Phase change chambers are divided into two identical parts by the air channel. The length of phase change chambers and air channel are individually designed as L_p = 37.5 mm and L_a = 20 mm, with the identical height of H_p = 500 mm. Besides, an electric fan is fixed at the outlet of air channel in order to drive air flow. When it comes to thermal energy storage media, organic paraffin wax having melting zone of 37 to 42 °C is selected as the PCM for the sake of producing sufficient heat transfer temperature difference between PCM and flowing air. The building interior is assumed as a closed uniform system and a constant relative humidity (RH) of 0.5 for indoor air will be utilized in this research. Thermophysical properties of PCM and moist air (calculated from EES) are illustrated in Table 1 [25,35].

2.2. Governing equations

2.2.1. PCM

Several reliable assumptions established to simplify theoretical modeling are listed as follows [36].

(1) Liquid PCM flow is regarded as incompressible laminar flow;
(2) PCM is subjected to thermal buoyancy and only the density variation conforms to the Boussinesq approximation;
(3) Liquid PCM belongs to the Newtonian fluid without volume change upon phase transition.

Liquid PCM gradually freezes into solid PCM and the stored thermal energy will be released into the indoor environment. In this scenario, enthalpy-porosity method is adopted to simulate the phase transition process. The whole computational domain is termed as a porous zone with porosity of each cell characterized by liquid fraction. Based on the above assumption, the governing equations of PCM in terms of continuity, momentum and energy conservation are shown in Eqs. (1)–(3) [13,37,38].

$$\frac{\partial(\rho_f)}{\partial\tau}+\nabla(\rho_f\vec{u})=0 \tag{1}$$

$$\frac{\partial(\rho_f\vec{u})}{\partial\tau}+\nabla\left(\rho_f\vec{u}\vec{u}\right)=-\nabla p+\mu_f\nabla^2u+S_u \tag{2}$$

$$\frac{\partial(\rho_f H)}{\partial\tau}+\nabla\left(\rho_f\vec{u}H\right)=\nabla(\lambda_f\nabla T)+S_r \tag{3}$$

where τ is the time; $\vec{u}$ is the velocity vector; ρ_f, μ_f, λ_f and p are the density, dynamic viscosity, thermal conductivity and pressure of PCM; $S_u=-A_{mushy}\frac{(1-\theta)^2}{\theta^3+\varphi}$, $A_{mushy}=10^5$, $\varphi=0.001$; θ is the volume fraction of liquid PCMs; S_r represents the source term in energy

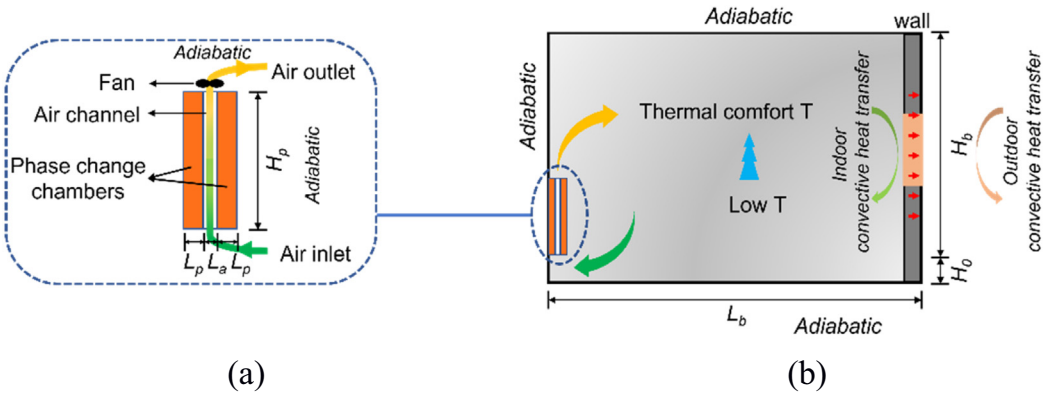

Fig. 1. Simplified physical model of studied building. (a) Active phase change heater; (b) Two-dimensional structure of the building.

Table 1
Thermophysical properties of PCM and moist air.

Properties	PCM		Moist air (RH = 0.5, at 25 °C) from EES
	Solid	Liquid	
Density ρ (kg/m^3)	860	820	1.165
Specific heat c_p(J/kg/°C)	1850	2050	1025
Thermal conductivity κ (W/m/°C)	0.28	0.17	0.02555
Viscosity μ (Pa·s)	–	0.032	0.00001846
Latent heat L (kJ/kg)	150		
Melting point T_m(°C)	37	42	
Thermal expansion β (1/°C)		0.000385	

conservation equation; H denotes the PCM enthalpy that is normally equal to the accumulation of sensible heat (h_s) and latent heat (L).

$$H = h_s + \theta L \tag{4}$$

$$h_s = h_{ref} + \int_{T_{ref}}^{T} c_{p_f} dT \tag{5}$$

where h_{ref} and T_{ref} are the reference enthalpy and temperature; c_{p_f} is specific heat of PCM. Liquid fraction of θ is used to reflect the volume proportion of PCM unsolidified during the research. $\theta = 0$ or 1 represents all PCMs are in solid or liquid state. θ will linearly change within the scope of 0 and 1 when PCM is within the mushy region.

$$\theta = \begin{cases} 0, T_f < T_s \\ \frac{T_f - T_s}{T_l - T_s}, T_s < T_f < T_l \\ 1, T_f > T_l \end{cases} \tag{6}$$

where T_s and T_l are the initial and terminal temperatures of PCM during melting zone.

2.2.2. Moist air

Moist air in the investigation can be separated into two groups according to the applications. The first group is the moist air working as heat transfer fluid in the active phase change heater, whereas the second group refers to the moist air existing in the building interior. The former moist air is believed as working under laminar flow and the correspondent governing equations are listed as follows [24,27].

$$\frac{\partial(\rho_a)}{\partial \tau} + \nabla(\rho_a \vec{u}) = 0 \tag{7}$$

$$\frac{\partial(\rho_a \vec{u})}{\partial \tau} + \nabla\left(\rho_a \vec{u}\vec{u}\right) = -\nabla p + \mu_a \nabla^2 u \tag{8}$$

$$\frac{\partial(\rho_a T)}{\partial \tau} + \nabla\left(\rho_a \vec{u} T\right) = \nabla(\lambda_a \nabla T) + S_r' \tag{9}$$

The convective heat transfer between moist air and PCMs can be recognized as internal convection with the calculation formulas emerged in Eqs. (10)–(11).

$$S_r' = -S_r = h(T_f - T_a) \tag{10}$$

$$\mathrm{h} = \begin{cases} \frac{\lambda_a}{D} 3.66 Re \le 2500 \\ \frac{\lambda_a}{D} 0.027 Re^{\frac{4}{5}} Pr^{\frac{1}{3}} \left(\frac{\mu_a}{\mu_s}\right)^{0.14} Re > 2500 \end{cases} \tag{11}$$

where D is the equivalent diameter of air channel; λ_a, μ_a, Re and Pr are the thermal conductivity, dynamic viscosity, Nusselt number and Prandtl number of moist air, respectively; T_f and T_a are the transient temperatures of PCM and moist air.

As for the latter group of indoor moist air, it is acquired from the available reference [39,40] that its flow belongs to the complicated turbulence that enables to rapidly homogenize interior temperature. Given that primary aims of this investigation are to assess capacity of the active phase change heater and related thermal performance of built buildings from the aspect of energy conservation, therefore the entire internal space is assumed as an isothermal domain with the transient mean temperature marked as the performance index. The related energy conservation equation can be obtained in Eq. (12).

$$\begin{aligned} \rho V c_p \frac{\partial T_r}{\partial \tau} = {} & \rho v_o A_o c_p \left(\bar{T}_0^n - T_{ref}\right) - \rho v_i A_i c_p \left(\bar{T}_i^n - T_{ref}\right) \\ & - h_{conv} A_{conv} (T_r^{n+1} - T_{amb}) \end{aligned} \tag{12}$$

where V is the indoor volume; v_i and v_o are the velocity for air flowing into and out of air channel; A_i and A_o are the inlet and outlet areas of air channel; $\bar{T}_i^n$ and $\bar{T}_0^n$ are the mean temperatures for air flowing into and out of air channel at n time; h_{conv} and A_{conv} are the convective heat transfer coefficient and area toward to an external wall.

$$h_{conv} = 1/\left(\frac{1}{h_i} + \frac{1}{R_{wall}} + \frac{1}{h_o}\right) \tag{13}$$

where h_i and h_o are indoor and outdoor convective heat transfer coefficients, 5.7 and 23 W/(m^2·°C); R_{wall} is equivalent thermal resistance of the exterior wall with a window, 0.8 (m^2·°C)/W.

2.3. Initial, boundary and operational conditions

2.3.1. Initial condition

Initial temperature of PCM is supposed as slightly higher than the melting point in order to assure that PCM is liquid prior to investigation. The initial indoor temperatures of 6, 8, 12 and 16 °C corresponding to various start occasions are examined to estimate the thermal performance of a building coupling with an active phase change heater.

(1) Cold start. The active phase change heater systems are operated to heat indoor environment at lower initial temperature (6 °C).
(2) Middle start. The indoor mean temperature rises to a higher level (8 or 12 °C) and the active phase change heater needs to continuously provide thermal energy to the indoor.
(3) Warm start. The mean indoor temperature (16 °C) is about to approach the default thermal comfort temperature zone.

2.3.2. Boundary conditions

It is supposed that the active phase change heater is well sealed by insulated materials, thus attaining adiabatic boundary condition except the inner surfaces contacting with flowing moist air as shown in Fig. 1. The moist air passing through the air channel is solved for viscous air flow under the boundary conditions of velocity-inlet and pressure-outlet. In terms of the building, only the right boundary is subjected to convective heat transfer with the ambient temperature fixed at 5 °C. The other walls including top, bottom and left sides are corresponding to adiabatic boundaries.

2.3.3. Operational condition

The object of this investigation is to improve indoor thermal environment of a building through the active phase change heater. Actually, it is apparent that the indoor temperature will gradually increase with the continues working of heater and may beyond the thermal comfort temperature range. Since overheated temperature is detrimental to human metabolic activity, reliable operational strategy should be developed to ensure the indoor temperature lie in thermal comfortable range. The following research adopts a thermal comfortable temperature range of 18 to 24 °C, which means that the working model is on when the indoor temperature is lower than 18 °C. While, the working model is off as long as the indoor temperature is larger than 24 °C. The shifting is substantially implemented by controlling the electric fan and the detailed operational models can be classified into the following types:

Model Ⅰ. When the indoor temperature is below 18 °C, the control signal will be on with the related air velocity of v_{set}, as shown in Eq. (14). The air velocity always exists until the indoor temperature exceeds 24 °C.

$$v_i = \left\{ \begin{array}{c} v_{set} implict \quad event1: \ T_r < 18 \ \ C \\ v_{set} implict \quad event2: \ \ 18 \leqslant T_r \leqslant 24 \ C \\ 0 \ implict \quad event3: \ \ T_r > 24C \end{array} \right\} \tag{14}$$

Model Ⅱ. When the indoor temperature is above 24 °C, the air velocity is approached to 0 owing to the turnoff of control signal. Eq. (15) indicates that the air velocity will change to v_{set} on condition that the indoor temperature is lower than 18 °C.

$$v_i = \left\{ \begin{array}{c} 0 \ \ implict \quad event1: \ T_r > 24 \ C \\ 0 \ implict \quad event2: \ \ 18 \leqslant T_r \leqslant 24 \ C \\ v_{set} \ \ implict \quad event3: \ \ T_r < 18 \ C \end{array} \right\} \tag{15}$$

where T_r is the transient indoor mean temperature; v_{set} and v_i are set velocity and actual velocity for moist air adopted in the active phase change heater, respectively.

2.4. Model solving and validation

2.4.1. Model solving

Three governing equations of continuity, momentum and energy conservation are firstly discretized by means of staggered grid technology within the computational region and then solved by the finite element method embedded in COMSOL Multiphysics. The free step backward differentiation formula controls the calculation time steps within a rational order and a parallel direct solver with a rational residual error is about to solve the residual equations. Convergence with relative residual of 10^{-5} for continuity equation, momentum equation and energy equation will be checked at each time step of the numerical calculation for purpose of maintaining a highly accurate resolution. When it comes to the operational events, the residual of 10^{-4} is selected to establish the switching of air velocity utilized in active phase change heaters.

2.4.2. Mesh independence

The unstructured grid method consisting of triangular elements is adopted in this calculation, since COMSOL owns the capacity of implementing adaptive remeshing. Mesh number is of crucial importance to the finite element method and thus its independency should be considered in detail prior to the numerical investigation. Four mesh numbers of 6485, 12573, 20,427 and 32,894 are checked in the mesh independency with the results plotted in Fig. 2.

Fig. 2 shows liquid fraction of PCM and indoor temperature as function of measured time under the air velocity of 0.20 m/s and initial temperature of 6 °C. It is perceived from Fig. 2 (a) and (b) that the PCM liquid fraction and indoor temperature are nearly overlapped when the mesh number is larger than 20427. Their results almost maintain unchanged with the continuous increase of mesh numbers. Whereas, the calculated process will take amounts of time on the condition of larger mesh numbers. Therefore, the mesh number of 20,427 is recommended based on dual considerations of computational accuracy and saving costs.

2.4.3. Model validation

Considering that few literatures related to the thermal performance of a building with active phase change heaters are available, validation of the built model is accomplished by the two parts: (1) Comparison between experiments and numerical calculation for the phase change unit containing targeted PCM. Constant heat flux of $\dot{q} = 4410 W/m^2$ is exerted in the corresponding experiments; (2) Comparison between literature results and numerical calculation for the phase change exchanger. Experiments conducted in Ref. [41] utilize a triplex tube heat exchanger as thermal energy storage. RT82 paraffin with melting peak temperature of 82 °C and water are separately employed as PCM and HTF. Initial temperatures of 87 and 68 °C for HTFs are utilized in the melting and solidification experiments. As indicated in Fig. 3 (a) and (b), temperatures of PCM obtained from built numerical model are in excellent agreement with experimental results of phase change unit or phase change exchangers having HTFs working at mass flow rates of 8 and 16 kg/min with the elapse of time. Slight discrepancy between calculated and experimental results might lie in difference between the real object and assumed physical model. It can be speculated from the comparable results that built theoretical model is accurate enough to be utilized in the following research.

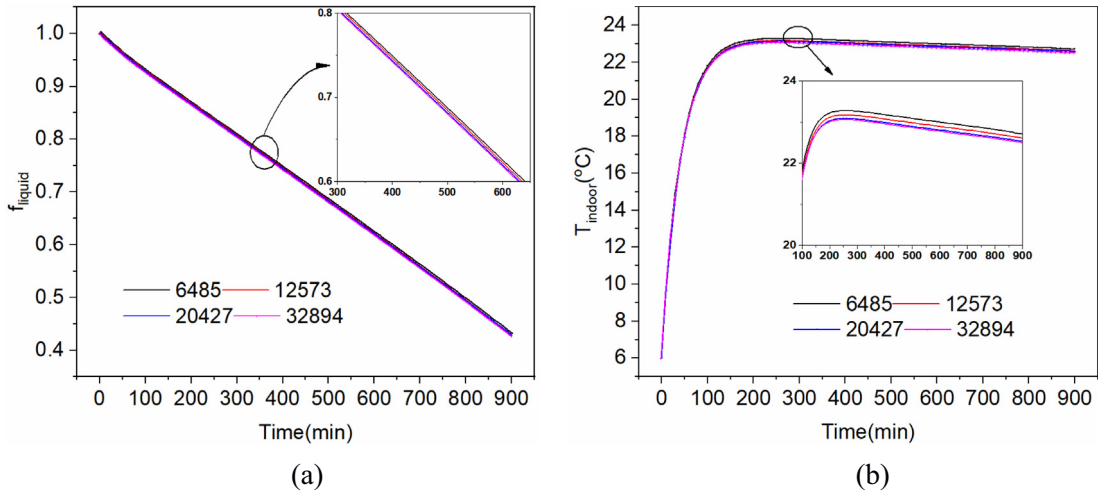

Fig. 2. Mesh independence of proposed numerical model. (a) Liquid fraction of PCM and (b) Indoor mean temperature.

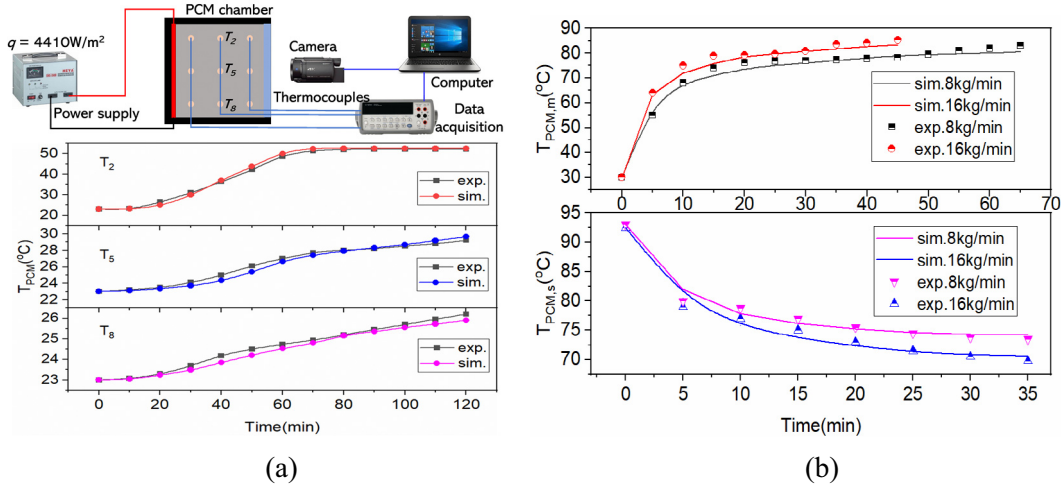

Fig. 3. Validation of the built model with experiments. (a) Phase change unit; (b) Phase change heat exchanger.

3. Results and discussion

3.1. System thermal performance and control

3.1.1. Indoor mean temperature

Indoor mean temperatures varied with air velocity are illustrated in Fig. 4. it is observed from Fig. 4 that mean temperatures enable to arrive the expected indoor temperature under any air velocity owing to introduction of active phase change heaters. It is also disclosed in Fig. 4 that lower initial temperature requires relatively longer operation time to reach the target temperature, in contrast to the higher initial temperature. Comparable results in Fig. 4 (a)-(f) indicate that large air velocity has capacity of supplying much thermal energy, bringing to active phase change heaters operating intermittently to control thermal comfortable temperature and frequent fluctuation of indoor mean temperature within the target zone of 18 to 24 °C. The larger the air velocity, the greater the fluctuation frequency of indoor mean temperature. Meanwhile, transient indoor mean temperature is found to present limited variation (always lower than 24 °C) when the air velocity is 0.20 m/s for initial temperatures of 6, 8, 12 and 16 °C. This sight is mainly attributed to the continuous operation of active phase change heaters to provide thermal energy for completing indoor thermal comfort.

3.1.2. Air outlet temperature

Moist air working as the HTF flows through active phase change heaters with the purpose of extracting thermal energy from phase change chambers. The acquired air temperatures at the outlet of air channel as function of air velocity are indicted in Fig. 5. It is obvious that there exist numerous rises and falls of air temperature at air velocities of 0.21 to 0.40 m/s and these fluctuations technically result from intermittent running of active phase change heaters. Moist air could gain more temperature fluctuations at larger air velocity compared to case at lower air velocity. Fig. 5 also indicates that air temperature increases quickly with the elapse of measured time at the initial stage. Air temperature climbs the upper temperature limit faster at higher initial temperature, in comparison to lower initial temperature cases. Whereas, the largest temperature of moist air at the outlet of air channel decreases with the augment of air velocity. Results of air temperatures are individually calculated up to 35.57, 35.39, 34.93, 34.36, 33.28 and 31.91 °C under conditions of 0.20, 0.21, 0.23, 0.25, 0.23 and 0.40 m/s. Moreover, the largest temperature of moist air changing limited with the vari-

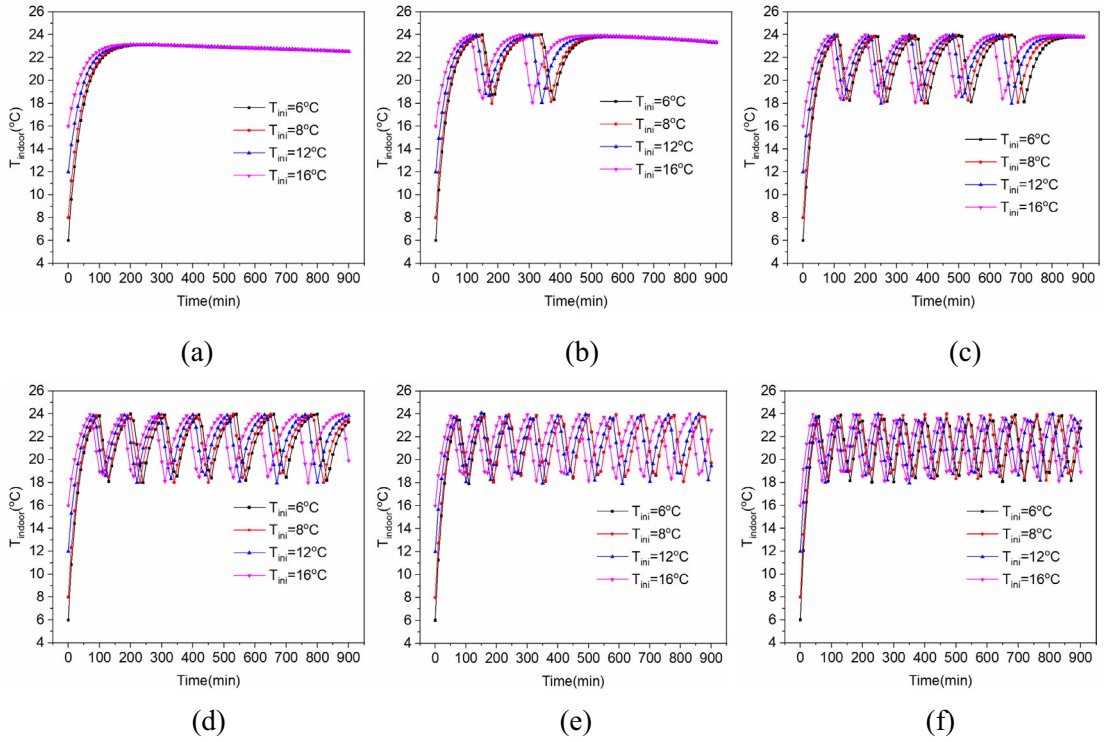

Fig. 4. Indoor mean temperature as function of air velocity. (a) 0.20 m/s; (b) 0.21 m/s; (c) 0.23 m/s; (d) 0.25 m/s; (e) 0.30 m/s and (f) 0.40 m/s.

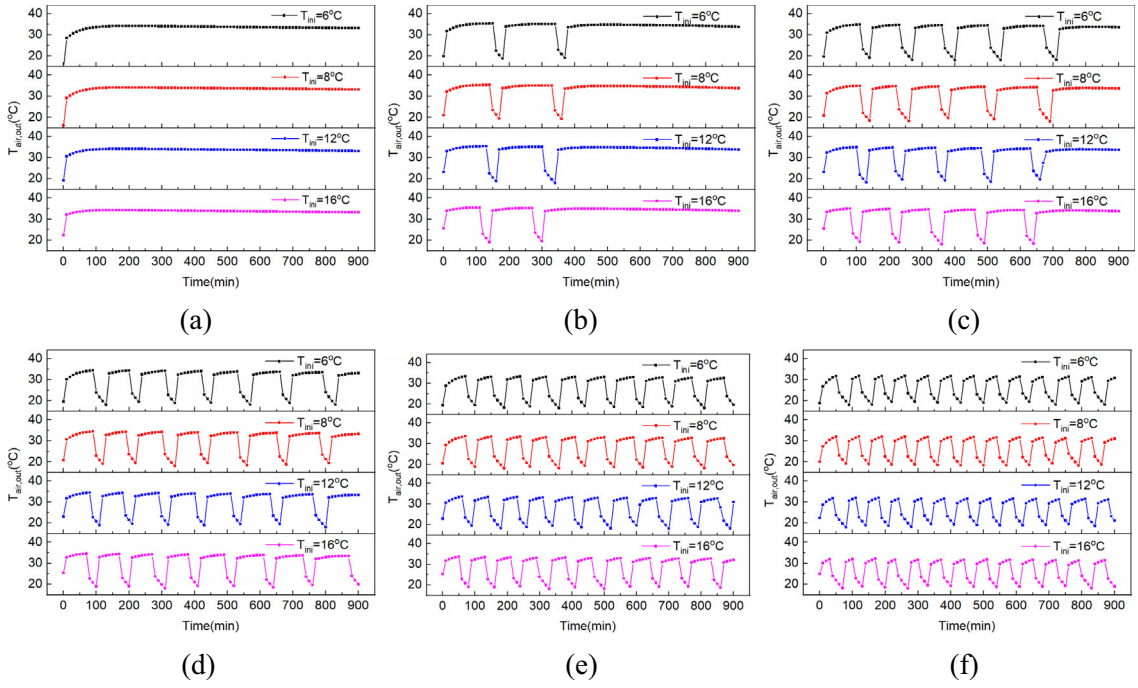

Fig. 5. Air outlet temperature variation as function of air velocity. (a) 0.20 m/s; (b) 0.21 m/s; (c) 0.23 m/s; (d) 0.25 m/s; (e) 0.30 m/s and (f) 0.40 m/s.

ation of measured time or initial temperature indicates that convective heat transfer between moist air and PCM has slight effect on overall heat transfer process.

3.1.3. Control and operation of active phase change heater

Based on the variation of indoor mean temperature and air out temperature in Figs. 4 and 5, it is rationally gained that active phase heaters will experience repetitive times of starting and ending during the investigation in order to maintain indoor thermal comfort temperature. Since working lifespan and running cost of active phase heaters are closely related to their operation, Fig. 6 exhibits control and operation of active phase change heaters. It is obtained that numbers of start-stop ascend quickly at the low velocity. When the low velocity rises to 3.0 m/s, effective start-

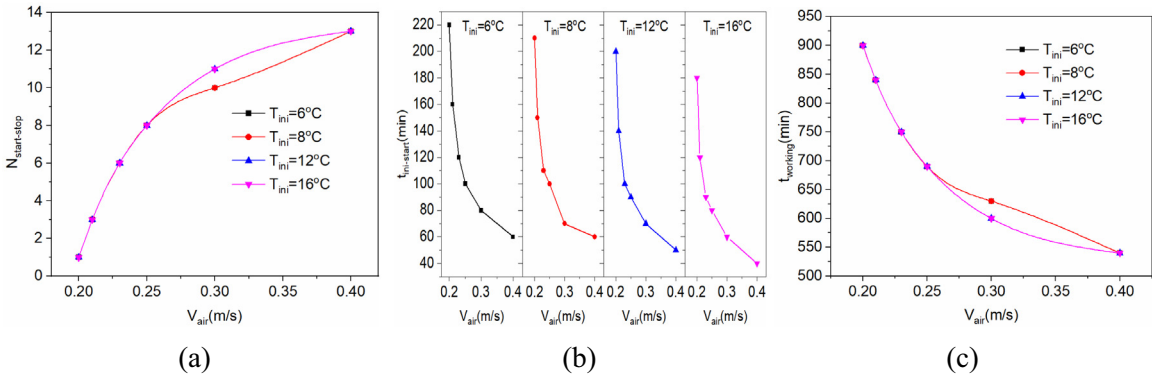

Fig. 6. Control and operation of active phase change heaters. (a) Number of start-stop, (b) First run time and (c) Total working time.

stop frequencies of active phase change heaters are determined as 10 times at lower initial temperatures (6 and 8 °C), 11 times at higher initial temperatures (12 and 16 °C). Whereas, continuing to increase air velocity brings to slight augment of start-stop frequency and the maximal results are found as 13 times for active phase change heaters running after 900 min.

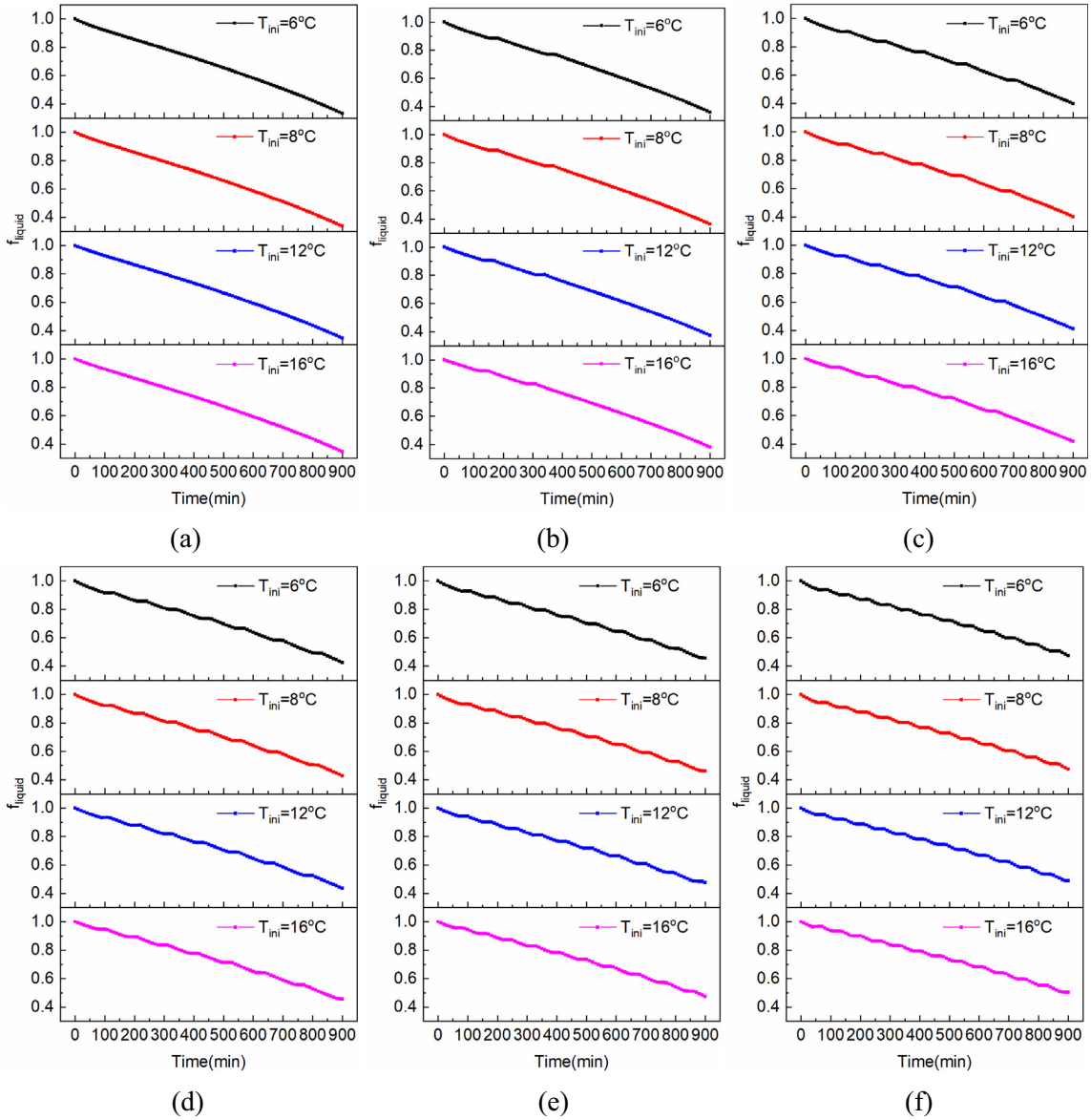

Fig. 7. Liquid fraction variation of PCM as function of air velocity. (a) 0.20 m/s; (b) 0.21 m/s; (c) 0.23 m/s; (d) 0.25 m/s; (e) 0.30 m/s and (f) 0.40 m/s.

Operation of active phase change heaters can be affected by the indoor initial temperature, especially for the first run. Fig. 6 (b) shows the first run time of active phase change heaters changed with air velocity. It is conceived that first run time drops significantly with the augment of air velocity for all operational cases. Comparable results also reveal that higher initial temperature enables to shorter the related first run time of phase change heater in contrast to lower initial temperature. The first run time is calculated as approximately 60, 60, 50 and 40 min for the initial temperatures of 6, 8, 12 and 16 °C, respectively. Fig. 6 (c) plots the total working times of active phase change heaters as function of air velocity during discharging process. It is obvious that the active phase change heaters need to continuously work (900 min) at the low velocity of 0.20 m/s. Total working times reveal parabolic downward trend with the augment of air velocity. When the air velocity rises to 0.40 m/s, the active phase change heaters possess approximately total working time of 540 min that is merely 0.6 of the entire investigated time.

3.2. Phase change heat transfer characteristics

3.2.1. Liquid fraction profile

Liquid PCMs substantially turn into solid as stored thermal energy is dissipated to indoor environment and the liquid fraction variations of PCM changed with air velocity are illustrated in Fig. 7. It is presented in Fig. 7 that liquid fractions of PCM display various declines with the elapse of time depending on the air velocity and initial temperature. For the air velocity of 0.20 m/s, Fig. 7 (a) indicates that liquid fraction of PCM decreases generally as increase of measured time. Meanwhile, there appears parallel stages in the liquid fraction of PCM as shown in Fig. 7 (b), which are corresponding to intermittent operation of active phase change heaters. Moist air no longer flows into the air channel and no thermal energy can be extracted in this respect. Therefore, liquid fractions of PCM remain unchanged during these unproductive periods. Similar phenomena can also be observed in Fig. 7 (c)-(f), indicating active phase change heaters have experienced multiple starts and stops during the investigation. It is further acquired that larger air velocity induces more parallel stages in terms of liquid fraction of PCM and more frequent of the intermittent operation of active phase change heaters. Fig. 7 indicates that liquid fractions of PCM change remarkably with air velocity rather than initial temperature. The final liquid fractions of PCM are still over 0 after 900 min, confirming that active phase change heaters perfectly satisfy the heating demand from studied building. It is calculated that liquid fractions drop down to approximately 0.332, 0.339, 0.399, 0.425, 0.457 and 0.473 at 900 min for air velocity of 0.20, 0.21, 0.23, 0.25, 0.30 and 0.40 m/s.

3.2.2. Phase change contour

Phase change contours of PCM incorporated in active phase change heaters changed with air velocity at various initial temperatures are illustrated in Fig. 8 and it is found that phase change contours demonstrate more noticeable variation along with air

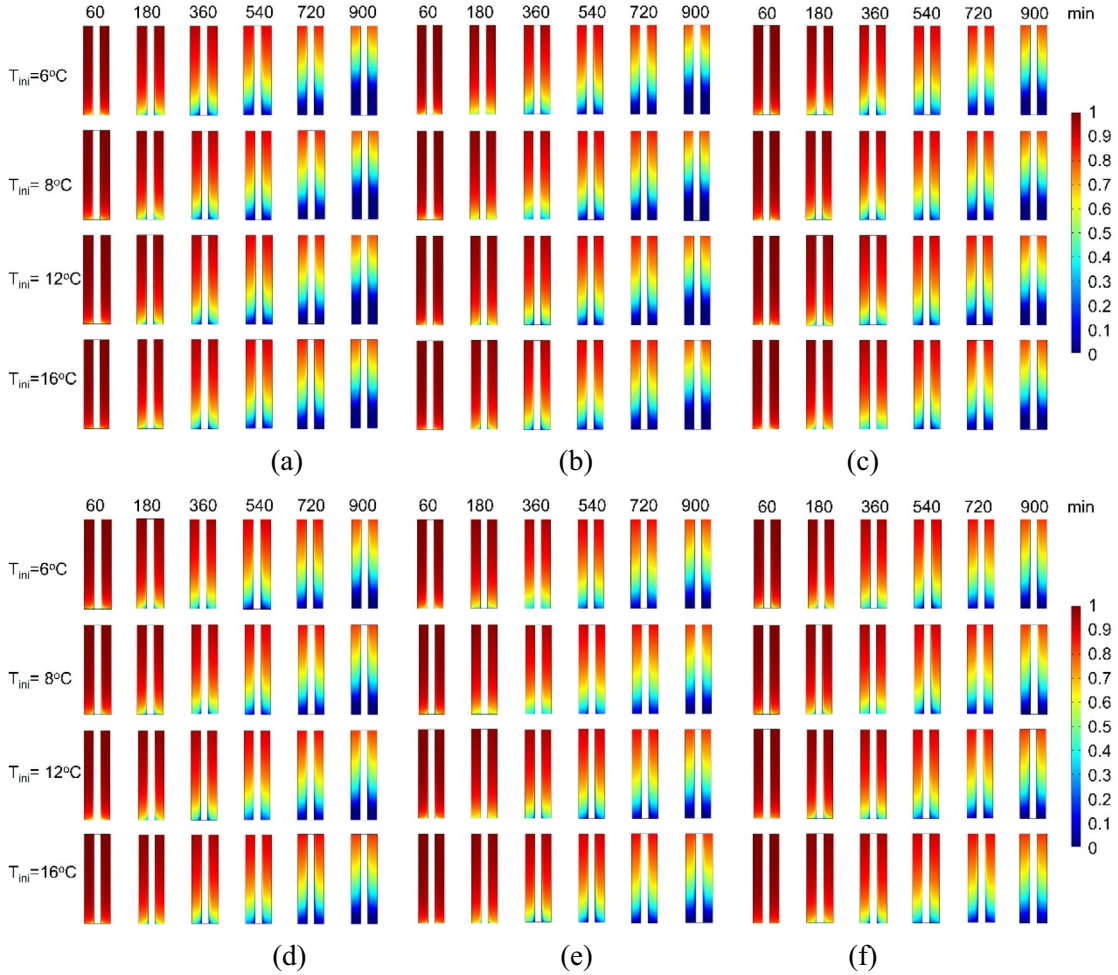

Fig. 8. Solid fraction of PCM in active phase change heaters as function of air velocity. (a) 0.20 m/s; (b) 0.21 m/s; (c) 0.23 m/s; (d) 0.25 m/s; (e) 0.30 m/s and (f) 0.40 m/s.

velocity rather than initial temperature. In any case of air velocity, phase change contours are almost constant with regards to various initial temperatures. This sight is attributed to the fact that thermal energy required from indoor environment to against heat loss varies slightly with air velocity, under thermal comfortable temperature zone. Phase change contours at measured times certify that there exist comparable lower liquid fractions along the walls of air channels, which well corresponds to the flowing of moist air. It is also indicated in Fig. 8 (a)-(f) that air velocity is capable of inducing remarkable non-uniformity in terms of phase change contours and therefore phase change chambers obtain more evident phase transition in horizontal direction at larger air velocities.

3.2.3. Temperature contour

Fig. 9 describes the temperature contours of PCMs in active phase change heaters and it is received that thermal energy is practically transferred from phase change chambers to central moist air flow. With the elapse of time, there appear obvious color changes at the bottom of phase change chambers that reflects intense heat exchanging performance. Thermal energy released from PCM is used to compensate heat loss to ambient, achieving comfortable thermal environment (18 ~ 24 °C). When it comes to temperature contours of moist air, it is connected with indoor environment, indicating its transient temperature identical to indoor temperature. Low-temperature (<18 °C) air flows into channels and then turns into high-temperature air when flowing out of channels. Under the indoor temperature within thermal comfort zone, it is observed in Fig. 9 (b)-(f) that constant results in temperature contours of moist air appear at several operating cases, such as 360 min with initial temperature of 6 °C. Suspension of active phase change heaters contribute to these sights to ensure indoor comfortable temperature. The significant temperature difference between the PCM and air channels further indicate that thermal resistance on the air side is responsible for the heat transfer limitation. Heat exchange rate between PCMs and moist air can be further improved by means of available strategies to reduce the thermal resistance on air side.

3.2.4. Velocity contour

Fig. 10 discloses the velocity contours of liquid PCM in active phase change heaters as function of air velocity. It is found that PCM velocity promoted by thermal buoyancy descends obviously with the elapse of time. Generally, the largest velocities appear in the lowest measured time and PCM gain maximal velocities of 1.85×10^{-4}, 1.86×10^{-4}, 1.87×10^{-4}, 1.89×10^{-4}, 1.91×10^{-4} and 1.92×10^{-4} m/s at 60 min at the air velocity of 0.20, 0.21, 0.23, 0.25, 0.30 and 0.40 m/s, respectively. After discharging time of 900 min, it is determined that velocities of liquid PCM drop down to merely 1.4×10^{-5}, 1.53×10^{-5}, 1.74×10^{-5}, 1.99×10^{-5}, 1.06×10^{-5}, 2.62×10^{-5} m/s under the air velocities of 0.20, 0.21, 0.23. 0.25. 0.30 and 0.40 m/s, respectively. On the basis of the velocity contours of liquid PCM circulating in the phase change chambers, it is deduced that PCM flow is crucial to its phase transition, then exerting unneglectable influence on related heat trans-

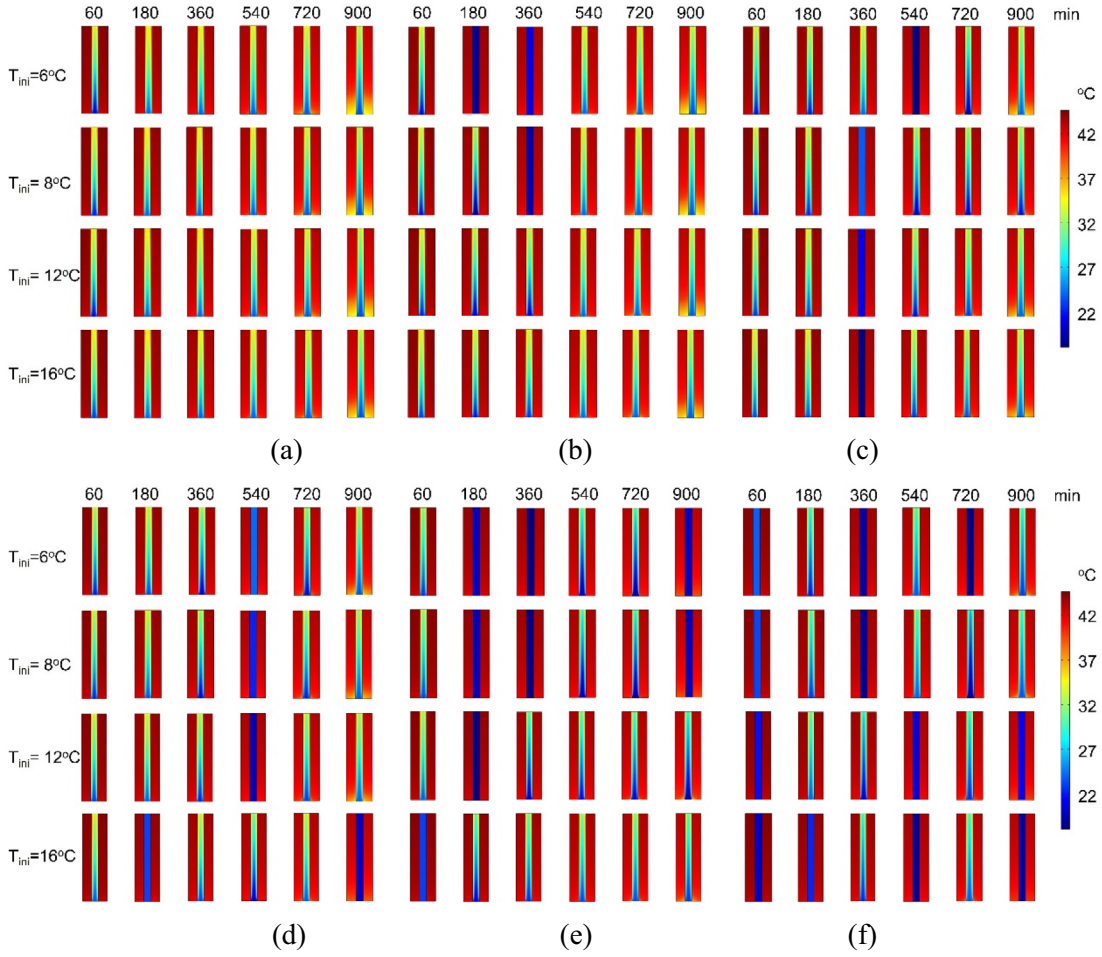

Fig. 9. Temperature contour of PCM and air in active phase change heaters as function of air velocity. (a) 0.20 m/s; (b) 0.21 m/s; (c) 0.23 m/s; (d) 0.25 m/s; (e) 0.30 m/s and (f) 0.40 m/s.

fer performance and temperature regulation of indoor thermal environment of buildings. Fig. 10 also reveals that there are no obvious changes in terms of velocity contours of liquid PCM under various initial temperatures.

3.3. Parametric analysis

The indoor temperature is expected to stay in the thermal comfort zone all the time. It is found that active phase change heaters work mostly at the warm start in practical applications which means the majority of thermal energy extracted from phase change heaters is utilized to balance against transient heat loss of indoor environment. Parameters of the active phase change heater enable to exert substantial effects on indoor thermal environment. Herein, parametric analysis is conducted under the operational conditions of initial temperature of 16 °C and air velocity of 0.30 m/s. Influences of four important parameters including thermal conductivity and melting point of PCM, ambient temperature and wall thermal resistance on system performance are evaluated in the following research.

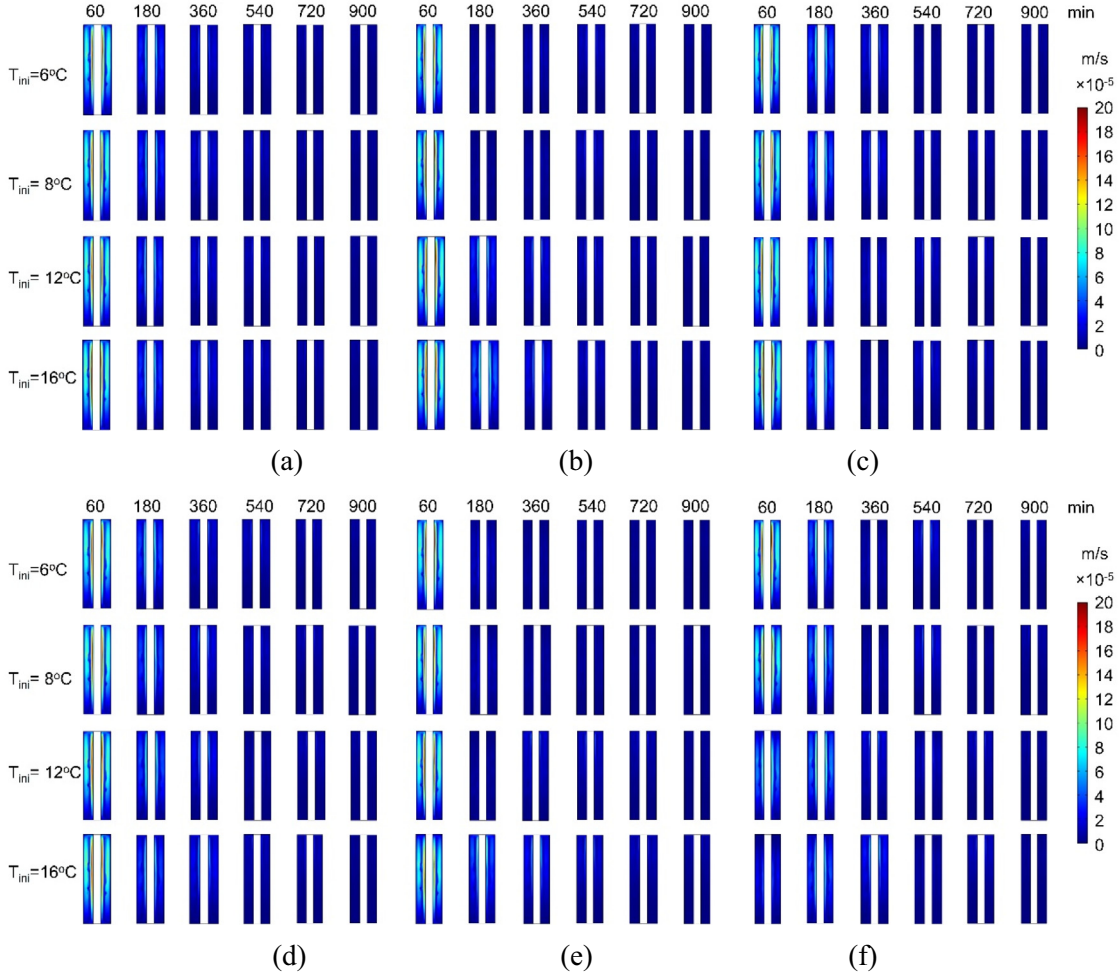

Fig. 10. Velocity contour of PCM in active phase change heaters as function of air velocity. (a) 0.20 m/s; (b) 0.21 m/s; (c) 0.23 m/s; (d) 0.25 m/s; (e) 0.30 m/s and (f) 0.40 m/s.

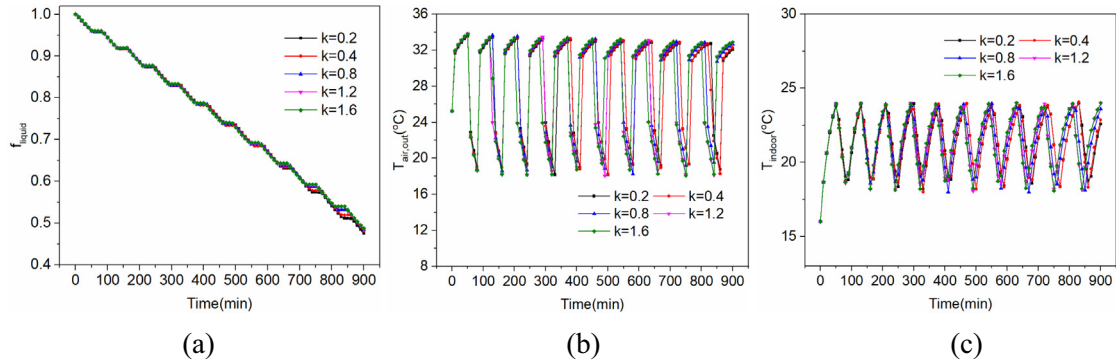

Fig. 11. Performance of proposed system as function of PCM thermal conductivity (v_{air} = 0.3 m/s, T_{ini} = 16 °C). (a) Liquid fraction of PCM; (b) Air outlet temperature and (c) Indoor temperature.

3.3.1. Thermal conductivity of PCM

Performance of proposed system as function of PCM thermal conductivity are plotted in Fig. 11 and it is observed that liquid fraction of PCM, air outlet temperature and indoor temperature vary limited with thermal conductivity of PCM, apart from the terminal stage. In consideration of air outlet temperature in Fig. 11 (b), it is discovered that larger thermal conductivity of PCM accelerates the heat transfer between PCM and flowing moist air, producing higher temperature air at the outlets. Accordingly, the liquid fraction of PCM and indoor mean temperature with larger thermal conductivity obtain slighter shifts compared to lower thermal conductivity as shown in Fig. 11 (a) and (c). Indoor mean temperature is always within the thermal comfort zone, which testifies that active phase change heater can meet building heating demand in this circumstance.

3.3.2. Melting point of PCM

Fig. 12 illustrates performance of proposed system as function of PCM melting point and it is exhibited that melting point of PCM has remarkable effect on the operational model of active phase change heaters. PCM with larger melting point stores more thermal energy and the heat releasing rate will also be enhanced to respond to heat load demand for indoor environment. Active phase change heaters need to work continuously to maintain suitable indoor temperature for lower melting point (30–36 °C) of PCM. whereas, higher melting points of PCMs (larger than 36 °C) qualify active phase change heaters to operate intermittently which can be found in Fig. 12 (a)-(c). Since PCM with melting temperature of 39 °C almost maintains the indoor temperature in highest level, it will consume most thermal energy and lowest liquid fraction of PCM can be perceived in Fig. 12 (a).

3.3.3. Ambient temperature

Ambient temperature is directly associated with heat loss between indoor and outdoor environment and performance of proposed system as function of ambient temperature is displayed in Fig. 13. It is comparably identified that ambient temperature is able to exert more noticeable influence on system performance, compared to thermal conductivity and melting point of PCM. The lower the ambient temperature, the larger the heat loss, the faster melting rate of PCM to maintain indoor thermal comfortable temperature. When low ambient temperatures (-10, −5 and 0 °C) are employed, the active phase change heaters continuously work to provide thermal energy and liquid fraction of PCM declines to merely 0.017, 0.095 and 0.196 at 900 min. The corresponding indoor temperature and air outlet temperature change mildly in this scenario. It can be hardly guaranteed that indoor temperature is within thermal comfort range for measured time larger than 670 min at ambient temperature of −10 °C. Large ambient temperatures (5 and 10 °C) decrease the heat loss and PCM individually gains high liquid fraction of 0.475 and 0.668 with satisfied guarantee of indoor objective temperature.

3.3.4. Thermal resistance of wall

Effects of thermal resistance for right wall on system performance are calculated and the obtained results are indicated in Fig. 14. It is shown that wall thermal resistance causes substantial fluctuations to indoor temperature, in spite of indoor temperature within thermal comfort range. Actually, thermal resistance of wall is identified as an important constant to heat loss. Larger thermal resistance induces slighter heat loss to ambient and the active phase change heater needs to work intermittently to prevent excessive indoor temperature. It is also apparent that no start-stop alternation occurs when wall thermal resistance is low (0.4

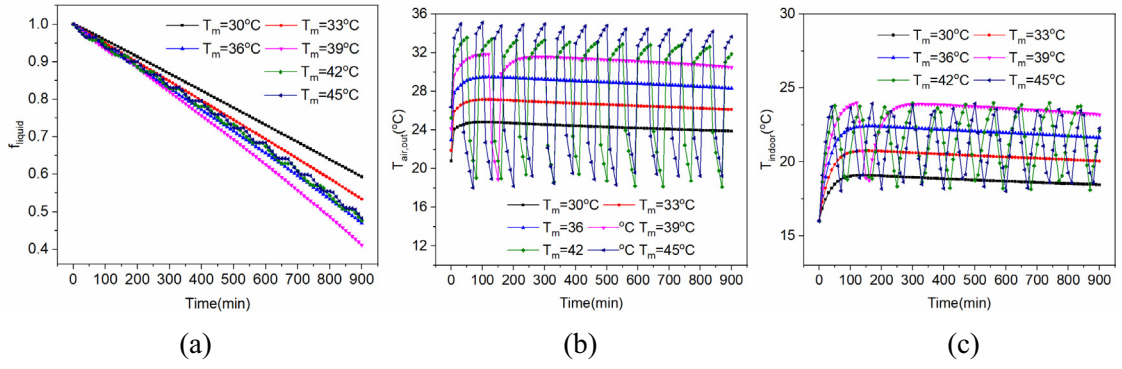

Fig. 12. Performance of proposed system as function of PCM melting point (v_{air} = 0.3 m/s, T_{ini} = 16 °C). (a) Liquid fraction of PCM; (b) Air outlet temperature and (c) Indoor temperature.

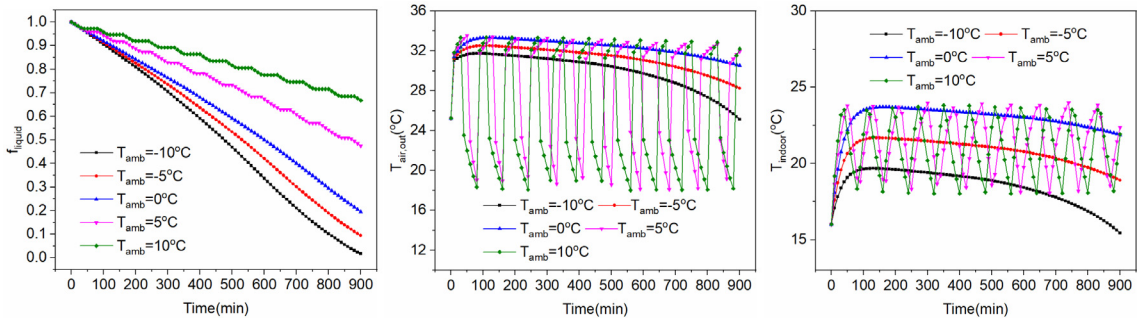

Fig. 13. Performance of proposed system as function of ambient temperature (v_{air} = 0.3 m/s, T_{ini} = 16 °C). (a) Liquid fraction of PCM; (b) Air outlet temperature and (c) Indoor temperature.

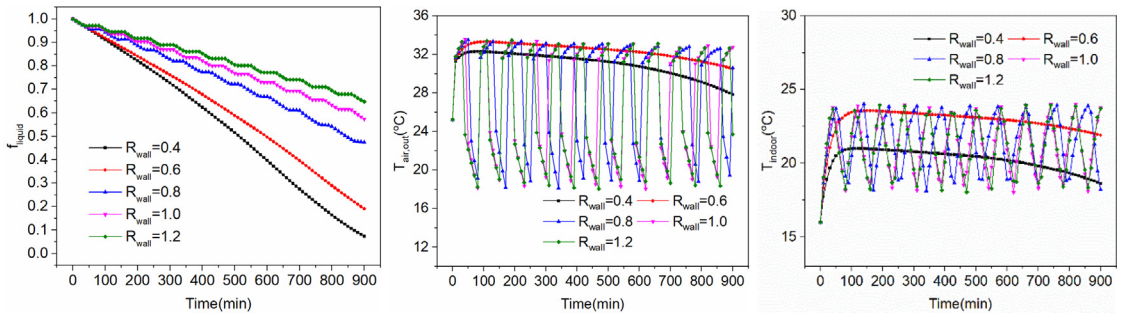

Fig. 14. Performance of proposed system as function of wall thermal resistance (v_{air} = 0.3 m/s, T_{ini} = 16 °C). (a) Liquid fraction of PCM; (b) Air outlet temperature and (c) Indoor temperature.

or 0.6 (m^2.°C)/W). Numerous start-stops can be observed in the operational model under the wall thermal resistance larger than 0.8 (m^2.°C)/W. The intermittent operations of active phase change heaters contribute to obvious fluctuations in terms of air outlet temperature and indoor temperature. Liquid fractions of PCM increase dramatically with the augment of wall thermal resistance. Finally, liquid fractions of PCMs fall down to 0.074, 0.190, 0.475, 0.575 and 0.647 for thermal resistance of 0.4, 0.6. 0.8, 1.0 and 1.2 (m^2.°C)/W, respectively.

4. Conclusions

An active phase change heater is proposed in order to satisfy heating demand from existing buildings with marine climate. Thermal energy with excess low-price electricity at off-peak tariff periods is charged into the system and then discharged at the on-peak tariff periods. Numerical model is built on basis of couple heat and mass transfer between PCM and indoor environment with indoor environment assumed as an isothermal domain. This paper adopted an event control to achieve switchable operations of active phase change heaters, maintaining a thermal comfort temperature zone at three starting occasions.

It is comprehensively inquired that indoor temperatures are generally within the expected range under various initial temperatures and air velocities. The largest temperatures of moist air at the channel outlets decrease gradually with the augment of air velocity. It is calculated that maximum of air outlet temperatures are 35.57, 35.39, 34.93, 34.36, 33.28 and 31.91 °C at velocity of 0.20, 0.21, 0.23, 0.25, 0.30 and 0.40 m/s, respectively. Active phase heaters work intermittently during the investigation in order to guarantee indoor thermal comfort temperature. Numbers of start-stop present parabolic increase while total working times decrease as air velocity rises from 0.20 to 0.40 m/s. The first run time can drop down to approximately 60, 60, 50 and 40 min for initial temperatures of 6, 8, 12 and 16 °C. Phase change heat transfer analysis indicates that liquid fractions of PCM decrease substantially with the elapse of studied time and several parallel stages occur owing to discontinuous operation of active phase change heaters. PCMs individually attain lowest liquid fraction of 0.347, 0.375, 0.411, 0.435, 0.475 and 0.489 for air velocities of 0.20, 0.21, 0.23, 0.25, 0.30 and 0.40 m/s after 900 min investigation. It is deduced that liquid flow is a crucial factor able to exert noticeable influence on PCM heat transfer characteristics and thermal regulation of indoor environment. Thermal resistance on the moist air side is the primary limit to heat transfer process. Parametric analysis reveals that PCM thermal conductivity is indecisive over melting point with regard to heat transfer of active phase change heaters. Ambient temperature and thermal resistance are identified as sensitive parameters and final liquid fraction of PCM can drop down to merely 0.074 under thermal resistance of 0.4 (m^2.°C)/W.

In conclusion, this novel active phase change heater provides a comparable strategy to meet the building heating demand from the perspective of energy dispatching and utilization, which is believed to be beneficial to accelerate the latent heat thermal energy storage applied in building energy conservation.

Data availability

Data will be made available on request.

Declaration of Competing Interest

The authors declare that they have no known competing financial interests or personal relationships that could have appeared to influence the work reported in this paper.

Acknowledgements

This work was supported by the National Natural Science Foundation of China (NO. 52108077 and 52006183), the Natural Science Foundation of Jiangsu Province (NO. BK20190860).

References

[1] A. Magrini, L. Marenco, A. Bodrato, Energy smart management and performance monitoring of a NZEB: Analysis of an application, Energy Reports. 8 (2022) 8896–8906, https://doi.org/10.1016/j.egyr.2022.07.010.
[2] R. Volpe, M. Gonzalez Alriols, N. Martelo Schmalbach, A. Fichera, Optimal design and operation of distributed electrical generation for Italian positive energy districts with biomass district heating, Energy Convers. Manag. 267 (2022) 115937. 10.1016/j.enconman.2022.115937.
[3] C. Bersani, A. Ouammi, R. Sacile, E. Zero, Model Predictive Control of Smart Greenhouses as the Path towards Near Zero Energy Consumption, Energies. 13 (2020) 3647, https://doi.org/10.3390/en13143647.
[4] S. Lu, Q. Lin, Y. Liu, L. Yue, R. Wang, Study on thermal performance improvement technology of latent heat thermal energy storage for building heating, Appl. Energy. 323 (2022), https://doi.org/10.1016/j.apenergy.2022.119594.
[5] R. Slabe-Erker, M. Dominko, A. Bayar, B. Majcen, K. Primc, Energy efficiency in residential and non-residential buildings: Short-term macroeconomic implications, Build. Environ. 222 (2022), https://doi.org/10.1016/j.buildenv.2022.109364.
[6] Z. Liu, Z.(. Yu, T. Yang, D.i. Qin, S. Li, G. Zhang, F. Haghighat, M.M. Joybari, A review on macro-encapsulated phase change material for building envelope applications, Build. Environ. 144 (2018) 281–294.
[7] Z.-G. Shen, S. Chen, B. Chen, Heat transfer performance of a finned shell-and-tube latent heat thermal energy storage unit in the presence of thermal radiation, J. Energy Storage. 45 (2022), https://doi.org/10.1016/j.est.2021.103724.
[8] Y. Wang, Q. Li, W. Miao, Y. Su, X. He, B. Strnadel, The thermal performances of cement-based materials with different types of microencapsulated phase change materials, Constr. Build. Mater. 345 (2022), https://doi.org/10.1016/j.conbuildmat.2022.128388.

[9] V.V. Tyagi, D. Buddhi, PCM thermal storage in buildings: A state of art, Renew. Sustain. Energy Rev. 11 (2007) 1146–1166, https://doi.org/10.1016/j.rser.2005.10.002.
[10] X. Jin, J. Yang, M. Li, G. Huang, A.C.K. Lai, Experimental and numerical study on the thermal energy storage performance of a novel phase-change material for radiant floor heating systems, Build. Environ. 223 (2022) 109491. 10.1016/j.buildenv.2022.109491.
[11] J. Dallaire, H.M. Adeel Hassan, J.H. Bjernemose, M.P. Rudolph Hansen, I. Lund, C.T. Veje, Performance analysis of a dual-stack Air-PCM heat exchanger with novel air flow configuration for cooling applications in buildings, Build. Environ. 223 (2022) 109450. 10.1016/j.buildenv.2022.109450.
[12] N.S. Bondareva, M.A. Sheremet, Heat transfer performance in a concrete block containing a phase change material for thermal comfort in buildings, Energy Build. 256 (2022), https://doi.org/10.1016/j.enbuild.2021.111715.
[13] A.I. Khdair, G. Abu Rumman, M. Basha, Developing building enhanced with PCM to reduce energy consumption, J. Build. Eng. 48 (2022), https://doi.org/10.1016/j.jobe.2021.103923.
[14] S. Zhang, Y. Ma, D. Li, C. Liu, R. Yang, Thermal performance of a reversible multiple-glazing roof filled with two PCM, Renew. Energy. 182 (2022) 1080–1093, https://doi.org/10.1016/j.renene.2021.11.008.
[15] N. Elawady, M. Bekheit, A.A. Sultan, A. Radwan, Energy assessment of a roof-integrated phase change materials, long-term numerical analysis with experimental validation, Appl. Therm. Eng. 202 (2022), https://doi.org/10.1016/j.applthermaleng.2021.117773.
[16] D.-I. Bogatu, O.B. Kazanci, B.W. Olesen, An experimental study of the active cooling performance of a novel radiant ceiling panel containing phase change material (PCM), Energy Build. 243 (2021), https://doi.org/10.1016/j.enbuild.2021.110981.
[17] L. Royon, L. Karim, A. Bontemps, Optimization of PCM embedded in a floor panel developed for thermal management of the lightweight envelope of buildings, Energy Build. 82 (2014) 385–390, https://doi.org/10.1016/j.enbuild.2014.07.012.
[18] F. Goia, E. Boccaleri, Physical–chemical properties evolution and thermal properties reliability of a paraffin wax under solar radiation exposure in a real-scale PCM window system, Energy Build. 119 (2016) 41–50, https://doi.org/10.1016/j.enbuild.2016.03.007.
[19] Y. Li, S. Liu, Experimental study on thermal performance of a solar chimney combined with PCM, Appl. Energy. 114 (2014) 172–178, https://doi.org/10.1016/j.apenergy.2013.09.022.
[20] J.C. Frutos Dordelly, M. El Mankibi, L. Roccamena, G. Remion, J. Arce Landa, Experimental analysis of a PCM integrated solar chimney under laboratory conditions, Sol. Energy. 188 (2019) 1332–1348, https://doi.org/10.1016/j.solener.2019.06.065.
[21] M. Alam, S. Devapriya, J. Sanjayan, Experimental investigation of the impact of design and control parameters of water-based active phase change materials system on thermal energy storage, Energy Build. 268 (2022), https://doi.org/10.1016/j.enbuild.2022.112226.
[22] Z. Jiang, P. Hlanze, J. Cai, Optimal predictive control of phase change material-based energy storage in buildings via mixed-integer convex programming, Appl. Therm. Eng. 215 (2022), https://doi.org/10.1016/j.applthermaleng.2022.118821.
[23] U. Stritih, P. Charvat, R. Koželj, L. Klimes, E. Osterman, M. Ostry, V. Butala, PCM thermal energy storage in solar heating of ventilation air—Experimental and numerical investigations, Sustain. Cities Soc. 37 (2018) 104–115, https://doi.org/10.1016/j.scs.2017.10.018.
[24] P. Charvát, L. Klimeš, M. Ostrý, Numerical and experimental investigation of a PCM-based thermal storage unit for solar air systems, Energy Build. 68 (2014) 488–497, https://doi.org/10.1016/j.enbuild.2013.10.011.
[25] J. Mazo, M. Delgado, J.M. Marin, B. Zalba, Modeling a radiant floor system with Phase Change Material (PCM) integrated into a building simulation tool: Analysis of a case study of a floor heating system coupled to a heat pump, Energy Build. 47 (2012) 458–466, https://doi.org/10.1016/j.enbuild.2011.12.022.
[26] O. Oruc, I. Dincer, N. Javani, Application of a ground source heat pump system with PCM-embedded radiant wall heating for buildings, Int. J. Energy Res. 43 (2019) 6542–6550, https://doi.org/10.1002/er.4791.
[27] H. Benli, A. Durmuş, Evaluation of ground-source heat pump combined latent heat storage system performance in greenhouse heating, Energy Build. 41 (2009) 220–228, https://doi.org/10.1016/j.enbuild.2008.09.004.
[28] K. Lin, Y. Zhang, X. Xu, H. Di, R. Yang, P. Qin, Experimental study of under-floor electric heating system with shape-stabilized PCM plates, Energy Build. 37 (2005) 215–220, https://doi.org/10.1016/j.enbuild.2004.06.017.
[29] K. Faraj, J. Faraj, F. Hachem, H. Bazzi, M. Khaled, C. Castelain, Analysis of underfloor electrical heating system integrated with coconut oil-PCM plates, Appl. Therm. Eng. 158 (2019), https://doi.org/10.1016/j.applthermaleng.2019.113778.
[30] M. Esen, A. Durmuş, A. Durmuş, Geometric design of solar-aided latent heat store depending on various parameters and phase change materials, Sol. Energy. 62 (1998) 19–28, https://doi.org/10.1016/S0038-092X(97)00104-7.
[31] M. Esen, T. Ayhan, Development of a model compatible with solar assisted cylindrical energy storage tank and variation of stored energy with time for different phase change materials, Energy Convers. Manag. 37 (1996) 1775–1785, https://doi.org/10.1016/0196-8904(96)00035-0.
[32] M. Esen, Thermal performance of a solar-aided latent heat store used for space heating by heat pump, Sol. Energy. 69 (2000) 15–25, https://doi.org/10.1016/S0038-092X(00)00015-3.
[33] X. Qiao, X. Kong, H. Li, L. Wang, H. Long, Performance and optimization of a novel active solar heating wall coupled with phase change material, J. Clean. Prod. 250 (2020), https://doi.org/10.1016/j.jclepro.2019.119470.
[34] X. Kong, C. Zhang, L. Guo, J. Ren, Operation optimization of a solar collector integrated with phase change material storage heating system, Energy Build. 275 (2022), https://doi.org/10.1016/j.enbuild.2022.112440.
[35] A. Gallardo, U. Berardi, Design and control of radiant ceiling panels incorporating phase change materials for cooling applications, Appl. Energy. 304 (2021), https://doi.org/10.1016/j.apenergy.2021.117736.
[36] X. Jin, X. Zhang, Thermal analysis of a double layer phase change material floor, Appl. Therm. Eng. 31 (2011) 1576–1581, https://doi.org/10.1016/j.applthermaleng.2011.01.023.
[37] D. Liang, M. Ibrahim, T. Saeed, A.M. El-Refaey, Z. Li, M.A. Fagiry, Simulation of a Trombe wall with a number of semicircular fins placed on the absorber plate for heating a room in the presence of nano-PCM, J. Build. Eng. 50 (2022), https://doi.org/10.1016/j.jobe.2022.104173.
[38] C. Nie, J. Liu, S. Deng, Effect of geometry modification on the thermal response of composite metal foam/phase change material for thermal energy storage, Int. J. Heat Mass Transf. 165 (2021), https://doi.org/10.1016/j.ijheatmasstransfer.2020.120652.
[39] M. Malayeri, M. Bahri, F. Haghighat, A. Shah, Impact of air distribution on indoor formaldehyde abatement with/without passive removal material: A CFD modeling, Build. Environ. 212 (2022), https://doi.org/10.1016/j.buildenv.2022.108792.
[40] A. Ameen, M. Cehlin, U. Larsson, H. Yamasawa, T. Kobayashi, Numerical investigation of the flow behavior of an isothermal corner impinging jet for building ventilation, Build. Environ. 223 (2022), https://doi.org/10.1016/j.buildenv.2022.109486.
[41] A.A. Al-Abidi, S. Mat, K. Sopian, M.Y. Sulaiman, A.T. Mohammad, Experimental study of melting and solidification of PCM in a triplex tube heat exchanger with fins, Energy Build. 68 (2014) 33–41, https://doi.org/10.1016/j.enbuild.2013.09.007.